A Density Functional Theory Based Protocol to Compute the Redox Potential of Transition Metal Complex with the Correction of Pseudo-Counterion: General Theory and Applications

Toru Matsui,*,[†] Yasutaka Kitagawa,[†] Yasuteru Shigeta,[‡,§] and Mitsutaka Okumura[†]

[†]Department of Chemistry, Graduate School of Science, Osaka University, 1-1 Machikaneyama, Toyonaka, Osaka 560-0043, Japan

[‡]Department of Materials Engineering Science, Graduate School of Engineering Science, Osaka University, 1-3 Machikaneyama, Toyonaka, Osaka 560-8531, Japan

[§]Core Research for Evolutional Science and Technology (CREST), Japan Science and Technology (JST) Agency, Kawaguchi, 332-0012 Saitama, Japan

S *Supporting Information*

ABSTRACT: We propose an accurate scheme to evaluate the redox potential of a wide variety of transition metal complexes by adding a charge-dependent correction term for a counterion around the charged complexes, which is based on Generalized Born theory, to the solvation energy. The mean absolute error (MAE) toward experimental redox potentials of charged complexes is considerably reduced from 0.81 V (maximum error 1.22 V) to 0.22 V (maximum error 0.50 V). We found a remarkable exchange-correlation functional dependence on the results rather than the basis set ones. The combination of Wachters+f (for metal) and 6-31++G(d,p) (for other atoms) with the B3LYP functional gives the least MAE 0.15 V for the test complexes. This scheme is applicable to other solvents, and heavier transition metal complexes such as $M_1(CO)_5(pycn)$ (M_1 = Cr, Mo, W), $M_2(mnt)_2$ (M_2 = Ni, Pd, Pt), and $M_3(bpy)_3$ (M_3 = Fe, Ru, Os) with the same quality.

$$G_{solv}^{corr} = G_{solv} - \frac{q^2}{2ar}\left(1 - \frac{1}{\varepsilon_r}\right) erf(\mu r \, |q|)$$
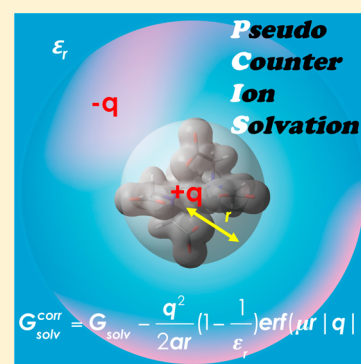
1. INTRODUCTION

Toward the design of new materials on a molecular level, it is helpful to understand the properties of a single molecule. The redox potential is one of the most fundamental quantities of transition metal complexes (TMCs), which clarifies whether the target molecule can easily take an electron or not. The importance of measuring the redox potential of TMCs is not limited to inorganic chemistry. The redox potential is one of the key pieces of information needed for a metal cluster to understand its catalytic property. It is also meaningful to investigate the redox potential of significant metallo-proteins, which play a crucial role in the electron transfer process in biomolecules. For example, a cytochrome *c*, which is a heme compound and contains an iron atom, is a mediator of electron transport processes in several biologically important systems. In order to understand the correlation between the structure and the redox potential of the metallo-enzymes, it requires accurate computation schemes from first principles.

Although many theoreticians have reported their methods[1−8] to compute the redox potential, the error from the experimental value is quite large, such as 0.20−0.30 V in mean absolute error (MAE). The deviation from the experimental values originates mainly from the treatment of the standard hydrogen electrode (SHE) potential, which has been treated as a constant and independent of the computational method in many theoretical papers. The international union of pure and applied chemistry (IUPAC) recommends the value 4.44 V as a SHE potential

observed by Trasatti.[9] Many theoretical[10−12] and experimental papers[13−17] reported various values ranging from 4.1 to 4.8 V depending on their experimental conditions, such as the temperature, electrode, and so on. From the view of theoretical/computational chemistry, it is also difficult to obtain the SHE potential, because this property needs the Gibbs free energy (GFE) of a proton in the aqueous phase. In order to avoid such problems, we also reported a new scheme for computing the SHE potential by combining experimental pK_a values of alcohol molecules and theoretical GFE with the polarizable continuum model (PCM) on the basis of our previous work for pK_a values.[18−21] We have calculated an absolute SHE potential of 4.52 V when we employed a gold-starndard calculation level as CCSD(T)/aug-cc-pVDZ. Our previous study for organic and inorganic molecules consiting of typical elements indicated that the value of the SHE potential depends on the computational methods, and we proposed a necessity for tuning of the SHE potential. The mean absolute error of the redox potentials became 0.1 V when we used a tuned SHE potential by using a popular density functional theory (DFT) such as B3LYP.

In spite of the success with the typical molecules, our previous scheme cannot describe TMCs with an excess charge. There remain two high barriers to achieve the accurate

computation of redox potentials of TMCs. One is a problem based on complicated electronic structure, which is typically seen in the first TMCs with multiple valence-charge and spin states. Because the electronic structures of both reduced and oxidized states play key roles in the redox potential, the well balanced static and dynamic electron correlation effects must be important. However, many theoretical papers have shown that the conventional −DFT can also reproduce the experimental ionization potential of metal complexes to some extent. Batista's group succeeded in reproducing the redox potential by using a PBE functional when they employed the redox potential of a ferrocene.[22] Recently, Solis and Hammes-Schiffer[23] computed the redox potential of cobalt dithiolene complexes, and their results agree very well with the experimental values. Hughes and Friesner[24] made a database set for redox potentials of the first TMCs and succeeded in calculating the redox potentials whose average error toward the experimental value is 0.12 ± 0.09 V by introducing seven empirical parameters obtained in their previous study.[25] Therefore, the results could be better when one chooses appropriate functionals of DFT and basis sets for transition metals. However, there is no fair rule to select the proper combination for a wide variety of the TMC when one does not have any experimental data.

The other barrier is the poor-description on the solvation energy of the metal complex with an excess positive/negative charge. A dielectric model such as PCM[26−29] has great success in describing a neutral reaction field and computing various properties in a solution. In fact, many theoretical papers have reproduced the experimental redox potential of almost neutral complexes. However, it is often said that these models do not estimate an accurate solvation energy of charged molecules. Due to this reason, a conventionally used solvation model overestimates/underestimates the redox potential of the positive/negative charged TMCs yet. Although an explicit counterion should be used for such an excess charged system, the results may depend on the position of the counterion, and it makes the matter more complicated. It is necessary to introduce some approximations for the purpose of avoiding these problems.

In this paper, we investigate the charge dependencies on the redox potential and propose a new method by putting an image counterion distribution around the TMC in order to neutralize the system. In section 2, we introduce the computational scheme. In section 3, we discuss the validities to use these schemes and show the application to famous TMCs. Finally, we give the conclusion in section 4.

2. COMPUTATIONAL DETAILS

In the conventional scheme, the redox potential has been obtained by using the Born−Haber cycle to obtain the GFE change in solution.[1] In our scheme, we directly compute the redox potential in solution, because we employ the result of geometry optimization and frequency analyses in the self-consistent reaction field. According to Nernst's law, the redox potential of a metal complex can be obtained by eq 1:

$$E_{redox} = \frac{G_{ox} - G_{red}}{F} - E_{SHE} \tag{1}$$

where $F = 23.06$ kcal mol^{-1} V^{-1} is the Faraday constant. G_{ox} and G_{red}, given in kcal mol^{-1}, are the GFEs of both the oxidized and reduced states of the TMCs in solution, respectively. Almost all computational papers that report the redox potential

of TMCs employ this equation. However, various SHE potentials, E_{SHE}, are employed, such as 4.28 V,[12] 4.43 V,[13] and so on. As shown later, this type of calculation scheme reproduces well the experimental redox potentials of weakly charged systems. On the other hand, it underestimates (overestimates) the redox potentials for excess positive (negative) systems. To overcome this problem, we put a "pseudo-counterion" (PCI) distribution whose net charge is $-q$ within a sphere with an effective radius R and added its solvation energy as a correction term. Corrected GFEs for both oxidized and reduced states in an atomic unit are shown in eqs 2a and 2b as

$$G_{ox}^{corr} = G_{ox} + G_{PCI,solv} = G_{ox} + \frac{q^2}{2R_{ox}}\left(1 - \frac{1}{\varepsilon_r}\right)\mathrm{erf}(\mu r_{ox}|q|) \tag{2a}$$

$$G_{red}^{corr} = G_{red} + G_{PCI,solv}$$
$$= G_{red} + \frac{(q-1)^2}{2R_{red}}\left(1 - \frac{1}{\varepsilon_r}\right)\mathrm{erf}(\mu r_{red}|q-1|) \tag{2b}$$

where ε_r and q are dielectric constant and the charge of the oxidized state, respectively. This solvation energy of PCI, $G_{PCI,solv}$, is based on the generalized Born (GB) theory. The error function corresponds to a scaling factor against the original GB which depends on the net charge in the long-range region, where the constant μ is a parameter describing a screening effect near TMCs.

Figure 1 depicts an illustration of the PCI correction. We set R_{ox} and R_{red} as effective radii for PCI in the oxidized and
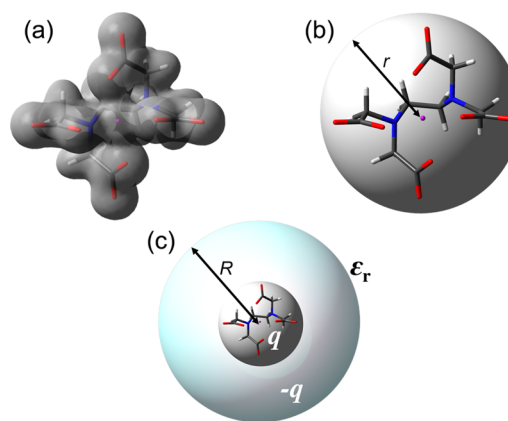

Figure 1. An illustrative representation of PCI. (a) We can define the cavity space in using the solvation model by setting the cavity model. (b) We approximated the cavity space as a sphere whose radius is r. (c) The radius of PCI R should be dependent on the value r. The dielectronic constant of this system is set to ε_r.

reduced states, respectively. We define V as the volume of the cavity for a given TMC at the optimized geometry when we employ PCM (see Figure 1a). We assume that the cavity is treated as a sphere with an approximate radius of r (see Figure 1b). The pseudo-counterion would be spread dependent on the size of the sphere, as seen in Figure 1c, so that R (R_{ox} or R_{red}) can be proportional to the approximate radius of the cavity sphere. Therefore, we can consider

$$R = ar = a\sqrt[3]{\frac{3V}{4\pi}} \quad (a = \text{const.}) \tag{3}$$

Table 1. Fitted Parameter for Each Functional and Mean Absolute Error (in V)

	conventional	previous		PCIS scheme				
	MAE^a	$E_{SHE,opt}{}^b$	MAE^c	a	μ	E_{SHE}	$R_{cor}{}^2$	MAE^d
B3LYP	0.53	4.08	0.34	12.65	0.0341	4.22	0.94	0.17
LC-BLYP	0.44	4.27	0.40	11.70	0.0317	4.42	0.91	0.20
PBE	0.83	3.67	0.36	16.40	0.1614	3.80	0.85	0.24
M06	0.54	4.24	0.46	5.84	0.0134	4.37	0.81	0.33

^{a}Using eq 8. ^{b}Using eq 9. ^{c}Using eq 7. ^{d}Using eq 5.

As the parameter "a" becomes larger, the correction term $1/2ar$ ($= 1/2R$) becomes smaller, and the effect of the correction for PCI becomes smaller. This means that the effect of charge correction gets smaller as the size of the system becomes larger. Similar to our previous study, we set E_{SHE} as a parameter, which depends on the computational methods. We called the series of calculation protocols "pseudo-counterion solvation" (PCIS) scheme.

When computing GFEs, one normally employs the vibrational analyses to obtain the normal modes and its vibrational partition function within the harmonic oscillator approximation. However, in many cases, the vibrational contributions to GFEs in both the oxidized and reduced states are almost the same, because the geometries are not so affected throughout the redox reaction. This also means that we can approximate $r_{ox} = r_{red} = r$. Actually, Friesner's group has shown that the addition of vibrational zero-point energy corrections and entropy effects are not so important.[1] We also have shown that the thermal effect is neglizible as an approximation to obtain a pK_a value.[21] In accordance with these papers, we consider $E_{ox} - E_{red}$ which corresponds to the adiabatic ionization potential (AIP) E_{AIP}. Instead, it is necessary to consider the formal condition 25 °C and 1 atm as a reference state, because we cannot consider the thermal effect within this approximation. Since 1 eV equals 23.06 (equal to the number F) kcal/mol, we obtain eq 4:

$$G_{ox} - G_{red} \approx E_{ox} - E_{red} \text{ (in kcal/mol)}$$
$$= FE_{AIP} \ (E_{AIP} \text{ in eV}) \tag{4}$$

Substituting eqs 2a, 2b, and 4 into eq 1, we obtain eq 5:

$$E_{redox} = E_{AIP} - \left\{ \frac{q^2}{2ar}\left(1 - \frac{1}{\varepsilon_r}\right)\text{erf}(\mu r|q|) - \frac{(q-1)^2}{2ar} \right.$$
$$\left. \times \left(1 - \frac{1}{\varepsilon_r}\right)\text{erf}(\mu r|q - 1|) + E_{SHE} \right\} \tag{5}$$

We evaluate the parameters appearing in eq 5 by using the experimental redox potential[30−45] and numerical E_{AIP} by a least-squares fitting. For simplicity, we employed 39 metal complexes as the test molecules as listed in the Supporting Information.

Throughout this study, we used the Gaussian 09 program package.[46] We employed the conductor-like polarizable continuum model (CPCM) with the PCI correction as a solvation model and universal force field (UFF), which is the default for Gaussian 09, as a model for the cavity space. All geometries are optimized for each density functional or basis set. The reference state is under the conditions of 25 °C (298.15 K) and 1 atm. In the Supporting Information, we only list the Cartesian coordinates of the optimized geometries of all compounds by the B3LYP functional.[47] Except for section 3.2, we employed B3LYP for the density functional, and Stuttgart/Dresden with the effective core potential (ECP) for metal

atoms and 6-31++G(d,p) for the other atoms (H, C, N, O, S, Cl) as a basis function.

3. RESULTS AND DISCUSSION

3.1. Validation of PCI Scheme to Charged Systems.
For the purpose of fitting the parameters, we rewrite eq 5 as follows:

$$E_{AIP} - E_{exp} = \frac{q^2}{2ar}\left(1 - \frac{1}{\varepsilon_r}\right)\text{erf}(\mu r|q|) - \frac{(q-1)^2}{2ar}$$
$$\times \left(1 - \frac{1}{\varepsilon_r}\right)\text{erf}(\mu r|q - 1|) + E_{SHE} \tag{6}$$

We here replaced the value E_{redox} with E_{exp} and employed the experimental value shown in ref 24. Detailed results are listed in the Supporting Information.

In this section, we present how much the redox potential depends on the net charge of the metal complexes.

In order to compare our new method with conventional methods, we introduce two computational schemes, the "conventional scheme" and the "previous scheme." In both schemes, the redox potential is written as

$$E_{redox} = E_{AIP} - E_{SHE} \tag{7}$$

In the "conventional scheme," we use a constant value of 4.44 V and employ the following equation:

$$E_{redox} = E_{AIP} - 4.44 \tag{8}$$

The other scheme employs the optimized $E_{SHE,opt}$, which minimizes the mean absolute error in test complexes. In order to minimize the mean absolute error $|E_{AIP} - E_{SHE} - E_{exp}|$, we fit the parameter $E_{SHE,opt}$ like eq 9.

$$E_{SHE,opt} = \overline{E}_{AIP} - \overline{E}_{exp} \tag{9}$$

which means the averaged value of $E_{AIP} - E_{exp}$. Applied to the computed results for 39 test compounds, we obtained the methodology dependent value of an "optimized" $E_{SHE,opt}$ for each computational method instead of E_{SHE} in eq 7. We call this computational scheme the "previous scheme."

Many papers on computational chemistry for TMCs have demonstrated benchmark calculations for DFT calculations. We picked up four popular functionals: B3LYP, PBE,[48] long-range corrected (LC)-BLYP,[49,50] and M06.[51]

Table 1 presents the dependencies of the corrected redox potentials on the exchange-correlation functional of DFT. As expected, the MAEs given by the "conventional scheme" are much larger than the other schemes in any computational methods. The MAE is at least 0.4 V with the other exchange-correlation functionals. PBE gives the worst MAE (0.83 V) among all of the methods. In some complexes, the error from the experimental value is larger than 1.5 V. This is due to the
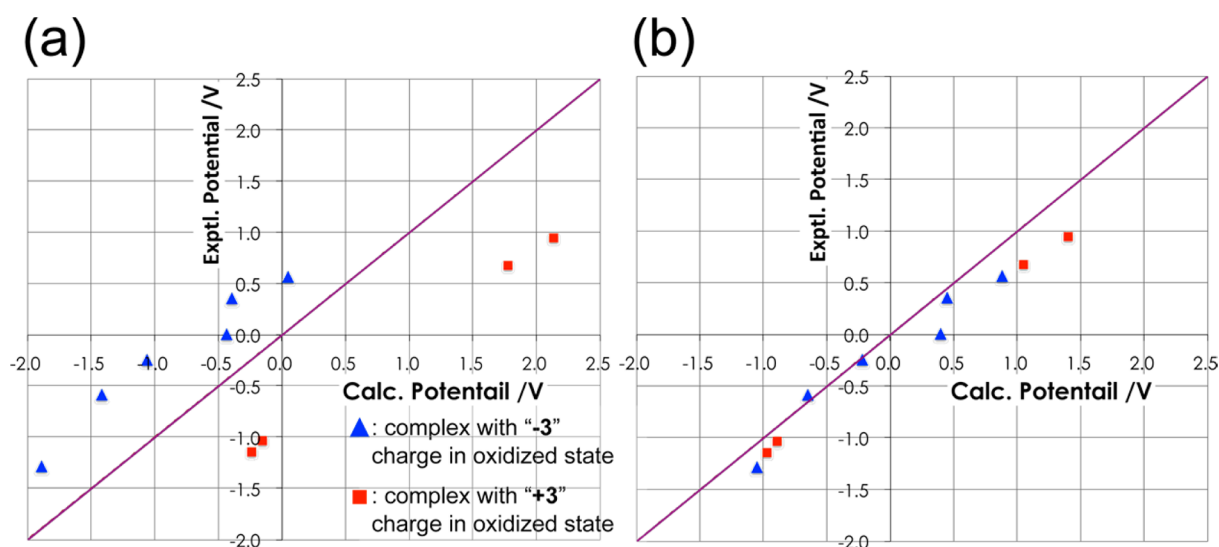
Figure 2. Correlation diagram of experimental vs computed redox potential of 10 charged compounds. When the plot is close to the purple line, the computed value agrees well with the experimental one. (a) Using normal computational scheme eq 7, which only shifts the SHE value. In using eq 7, we employed the "previous scheme." (b) Results given by the PCIS scheme (eq 5).

Table 2. Fitted Parameter of Each Combination for Basis Set and Mean Absolute Error (in V)

			previous		PCIS scheme				
	metal	others	$E_{SHE,opt}{}^a$	MAE^a	a	μ	E_{SHE}	$R_{cor}{}^2$	MAE^b
BS A	SDD	6-31G(d)	3.71	0.46	10.16	0.0537	3.91	0.94	0.16
BS B	SDD	6-31++G(d,p)	4.08	0.34	12.65	0.0341	4.22	0.94	0.17
BS C	LanL08(f)	6-31++G(d,p)	4.08	0.36	11.83	0.0335	4.23	0.93	0.17
BS D	Wachters+f	6-31++G(d,p)	4.03	0.33	13.33	0.0394	4.17	0.95	0.15
BS E	aDZ+DK^c	6-31++G(d,p)	3.98	0.35	12.81	0.0367	4.12	0.94	0.17

^{a}Using eqs 7 and 9. ^{b}Using eq 5. ^{c}We employed the basis function "aug-cc-pVDZ with Douglas−Kroll correction."

underestimation of the adiabatic ionization potential with pure functionals.

In the "previous scheme," the MAE is somewhat improved, especially in the PBE functional. On the other hand, the results are not so improved in LC-BLYP and M06, because the values of $E_{SHE,opt}$ are not so different from 4.44 V in such functionals. Although B3LYP gives the best results among the four computational methods, the MAE is no less than 0.34 V so far.

When we employ the "PCIS scheme," the errors are considerably decreaced in all computational methods. B3LYP gives the least MAE whereas M06, on the other hand, presents the largest MAE among these functionals within our treatment. Detailed results are shown in Tables S1 and S2 in the Supporting Information. Judging form the fitted value a, the correction based on the net charge is not so necessary. A pure functional such as PBE gives a small E_{SHE} value such as 3.85 V, whereas the hybrid functional and the functional with LC give higher E_{SHE} values. For example, B3LYP presents 4.22 V, which is very close to 4.28 V reported by Isse and Gennaro.[12] Limited to weakly charged systems (ranging from −1 to +1 in oxidized state), the correction for PCI is so small that using the constant SHE of 4.28 V does not cause fatal errors.

The parameters a and μ depend on the computational methods. In PBE, the fitted μ is very large, because the scaling factor works well in using PBE. M06 presents a small value for a, which may be caused by the poor description of electronic structure. The determination coefficient $R_{cor}{}^2$ is very large, 0.94, for B3LYP, whereas it is somewhat small for PBE and M06.

According to these results, the functional which includes both short-range and long-range correction will be a promising functional for presenting the least MAE in these test TMCs. In this study, we employed the B3LYP functional for further calculations because this functional gives the least MAE in this study.

In order to show the efficiency of the PCIS scheme in charged complexes, the experimental and computed redox potential is plotted in Figure 2. This figure reveals the significant change due to the charge-dependent correction. When we applied a "constant" SHE potential and eq 7, the error was very large, shown in blue triangles and red rectangles in Figure 2a. The mean absolute error (MAE) is 0.81 V, with the maximum error being +1.18 V for $Ni(tacn)_2$ by means of the previous scheme. When we applied the PCIS scheme (eq 5), the MAE was dramatically decreased to 0.20 V with the maximum error being +0.46 V for $Ni(tacn)_2$. The results with the PCIS correction are shown in Figure 2b. It is obvious that the PCIS scheme works well for describing the excess charged systems.

3.2. Basis Set Dependency. In the redox reaction of TMCs, the metals should be the main character so that the qualities of computational results strongly depend on the basis set for them. In this section, we investigated the basis set dependencies and discussed two issues: (1) which combination of basis function for metal and other ligands is appropriate for further calculations and (2) whether ECP influences the results for redox potential or not.

The results for fitted parameters and the MAE for each combination of basis sets are given in Table 2. We also show the detailed results in Table S3 of the Supporting Information. In any case, the PCIS scheme does not strongly depend on the basis set employed here judging from MAE and R_{cor}^2, because the difference of MAE is no more than 0.2 V. The roughest combination, BS A (SDD+6-31G(d)), presents a quite small SHE and a large μ. This large μ improves the results, because the "previous scheme" with BS A presents poor results (MAE = 0.45 V). BS C, which includes the Lanl08(f)[52] basis set, also gives good results. Furthermore, BS D (Wachters+f[53,54] for metal and 6-31++G(d,p) for other atoms) presents the best result, whose MAE is 0.15 V with eq 5. These results indicate that including the f polarization function for the metals is necessary for quantitative calculations of the redox potential of TMCs, especially when using eq 5.

On the other hand, the largest basis set combination, BS E, which employs the relativistic Douglas–Kroll–Hess correlated consistent basis sets aug-cc-pVDZ+DK[55] (denoted aDZ+DK in Table 2), does not improve as expected within the presented functional. This means that the diffuse function of the metal atom is not so important within the PCIS scheme. Judging from the difference between BS C and BS D, the choice of ECP or all electrons basis set does not so affect the redox potential. These results indicate that we can employ the PCIS scheme for heavier TMCs with a basis set with ECP.

3.3. Applications to Other Systems. The test molecules we used here have common points, which are six-coordinate systems and are observed in aqueous solution. In order to investigate the validity of using various TMCs in other environments, we should check two things. The first is whether we can apply the PCIS scheme to the other solvent and/or other coordination systems or not. Because we approximate the PCI as a sphere, we need to check whether the fitted parameter is appropriate for the other coordination system, such as planar four-coordination, or not. The second is to check the applicability to the heavier TMCs. As shown in the previous section, we have proven that using ECP does not affect the redox potential so that we can employ the PCIS scheme to the second or third TMCs. We employed B3LYP/BS B in this section. In particular, we investigated the following TMCs shown in Figure 3.

3.3.1. Other Solvents and Coordination Systems. At first, we examined seven compounds, $M(acac)_3$ (M = V, Cr, Mn, Fe, and Co) in acetonitrile and $V^{V/IV}(mnt)_3$ in dichloromethane as tests for using the PCIS scheme in the other solvents.

Table 3 lists the results for the seven compounds and corresponding experimental results. The computed values agree well with the experimental redox potential of $M(acac)_3$. Our scheme reproduces well the experimental redox potential of $V(mnt)_3$ even in the solvation with low ε_r, such as dichloromethane ($\varepsilon_r = 8.93$).

In the next step, we applied our scheme to the four-coordinated complexes. As the test molecules, we employed cobalt complexes such as $Co(bdt)_2$, which have been receiving much attention as a hydrogen evolving catalysts,[56] for which Solis and Hammes-Schiffer[23] have already computed the redox potential. Our computational scheme is still effective even for these four-coordinated systems, because we also reproduced the experimental value with presented parameters except for $Co^{II/I}(mnt)_2$. When we employed the quintet state as the reduced state, which is less stable than triplet state in 11.3 kcal/mol, we reproduced the experimental value for this compound.
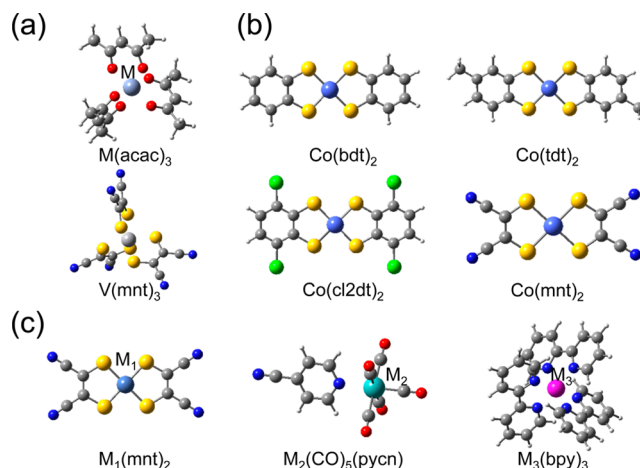

Figure 3. The optimized structure of each complex used in section 3.3. (a) $M(acac)_3$ and $V(mnt)_3$, (b) cobalt complexes, and (c) $M_1(mnt)_2$, $M_2(CO)_5(pycn)$, and $M_3(bpy)_3$. Carbon, sulfur, chloride, oxygen, nitrogen, and hydrogen are shown in gray, yellow, green yellow, red, blue, and white, respectively.

This error might be caused by the description of the electronic structure by B3LYP. These results indicate that the control of the value E_{SHE} which depends on the computational method is more important than the parameter of a radius for PCI.

3.3.2. Heavier Transition Metals. As our computational scheme uses ECP, we can apply it to heavier TMCs than the first TMCs.

As shown in Table 4, the results agree well with the experimental value. In the case of $M_1(mnt)_2$ (M_1 = Ni, Pd, Pt)[57] and $M_2(CO)_5(pycn)$ (M_2 = Cr, Mo, W),[58] no systematic error is found, and MAE is also less than 0.25 V. These results support the PCIS scheme being applicable to heavier TMCs once we obtained the parameter from the test first TMCs. The reason why the PCIS scheme works well for them might be the error cancellation between the oxidized and reduced states. Therefore, the results will be almost smilar at the same calculation level.

In the case of the larger molecule $M_3(bpy)_3$ (M_3 = Fe, Ru, Os),[59,60] on the other hand, we underestimated the redox potential compared with the experimental value especially in $Fe(bpy)_3$. We found that such an underestimation is due to the lack of the polarization function in the presented computational scheme. When we applied BS E (aDZ+DK and 6-31++G(d,p)), the computed redox potential was improved to +0.87 V for $Fe^{III/II}(bpy)_3$. On the other hand, we almost reproduce the redox potential of other elements.

4. CONCLUSION

We proposed the PCIS scheme to compute the redox potential of TMCs with the correction of solvation energy especially for the excess charged systems. The effect of the counterion distribution around TMCs can be approximated by the solvation energy depending on the size and charge of TMCs. Although the test calculations for fitting the parameters are limited to six-coordinated complexes in the aqueous phase, our scheme is widely applicable to the other solvent coordination systems, even to the heavior transition metals. The mean absolute error of the test TMCs is at least 0.15 V with B3LYP, which considerably improved the results of the previous scheme. Moreover, this PCIS scheme can accurately give the redox potential of TMCs with +3/−3 charge qualitatively.

Table 3. Computed Redox Potential (in V) for Test Calculations in Other Solvent

	solvent	charge[a]	calcd.[b] − exptl.	calcd.[c] − exptl.	exptl.
$V(acac)_3$	CH_3CN	0	0.08	0.26	−1.18
$Cr(acac)_3$	CH_3CN	0	−0.20	−0.03	−1.57
$Mn(acac)_3$	CH_3CN	0	0.06	0.24	0.15
$Fe(acac)_3$	CH_3CN	0	0.25	0.43	−0.43
$Co(acac)_3$	CH_3CN	0	0.28	0.46	−0.11
$V^{V/IV}(mnt)_3$	CH_2Cl_2	−2	0.05	0.03	−0.32
$Co^{III/II}(bdt)_2$	H_2O/CH_3CN^d	−1	0.00	−0.01	−0.39[e]
$Co^{III/II}(tdt)_2$	H_2O/CH_3CN^d	−1	−0.05	−0.07	−0.45[e]
$Co^{III/II}(Cl_2dt)_2$	H_2O/CH_3CN^d	−1	0.03	0.01	−0.26[e]
$Co^{II/I}(mnt)_2$	H_2O/CH_3CN^d	−2	0.36 (−0.13[f])	0.07 (−0.42[f])	−1.24[e]

[a]The net charge of "oxidized" state. [b]Using the "PCIS scheme" (eq 5). [c]Using the "previous" scheme (eq 7). [d]We set $\varepsilon_r = 50.0$ as the mixed solvent of H_2O/CH_3CN. [e]We converted the reported value to vs SHE in V. [f]Result is given by the quintet state in the reduced state.

Table 4. Computed Redox Potential (in V) of Heavier TMCs

	solvent	charge[a]	calcd.[b] − exptl.	calcd.[c] − exptl.	exptl.
$Ni^{III/II}(mnt)_2$	CH_3CN	−1	−0.04	−0.05	0.47[d]
$Pd^{III/II}(mnt)_2$	CH_3CN	−1	−0.04	−0.04	0.68[d]
$Pt^{III/II}(mnt)_2$	CH_3CN	−1	0.02	0.00	0.47[d]
$Cr^{III/II}(CO)_5(pyCN)$	CH_3CN	0	−0.26	−0.08	−0.98[d]
$Mo^{III/II}(CO)_5(pyCN)$	CH_3CN	0	−0.23	−0.05	−0.98[d]
$W^{III/II}(CO)_5(pyCN)$	CH_3CN	0	−0.22	−0.04	−0.93[d]
$Fe^{III/II}(bpy)_3$	CH_3CN	+3	−0.27	0.38	1.03
$Ru^{III/II}(bpy)_3$	CH_3CN	+3	−0.27	0.39	1.24
$Os^{III/II}(bpy)_3$	CH_3CN	+3	−0.12	0.54	0.84
$Co^{III/II}(bpy)_3$	water	+3	−0.14	0.52	0.31

[a]The net charge of oxidized state. [b]Using the "PCIS scheme" (eq 5). [c]Using the "previous scheme" (eq 7). [d]The reported value is shown in vs SCE so we added 0.244 V for vs SHE value.

However, the computed SHE potential is quite different from the one obtained by our previous study. Only LC-BLYP avoids such a discrepancy, which may be related to the good description of an orbital energy with the LC scheme reported by Tsuneda et al.[61] Although the choice of functional of DFT is more important than that of the basis set, a polarization function for the metal atom can reduce the MAE. This computational scheme will be a promising computational tool for investigating the redox potential of metal clusters, biological molecules, and designing new materials and catalysts, and so on.

ASSOCIATED CONTENT

Ⓢ Supporting Information

Supporting Information includes the information on details for benchmark molecules, Tables 1 and 2, and optimized geometry of each compound by B3LYP/BS B. This material is available free of charge via the Internet at http://pubs.acs.org.

AUTHOR INFORMATION

Corresponding Author

*E-mail: matsui@chem.sci.osaka-u.ac.jp.

Notes

The authors declare no competing financial interest.

REFERENCES

(1) Baik, M.-H.; Friesner, R. A. *J. Phys. Chem. A* **2002**, *106*, 7407.
(2) Uudsemaa, M.; Tamm, T. *J. Phys. Chem. A* **2003**, *107*, 9997.
(3) Shimodaira, Y.; Miura, T.; Kudo, A.; Kobayashi, H. *J. Chem. Theory Comput.* **2007**, *3*, 789.
(4) Roy, L. E.; Batista, E. R.; Hay, P. J. *Inorg. Chem.* **2008**, *47*, 9228.
(5) Takano, Y.; Nakamura, H. *Int. J. Quantum Chem.* **2009**, *109*, 3583.
(6) Migliore, A.; Sit, P. H.-L.; Klein, M. L. *J. Chem. Theory Comput.* **2009**, *5*, 307.
(7) Takano, Y.; Yonezawa, Y.; Fujita, Y.; Kurisu, G.; Nakamura, H. *Chem. Phys. Lett.* **2011**, *503*, 296.
(8) Jono, R.; Sumita, M.; Tateyama, Y.; Yamashita, K. *J. Phys. Chem. Lett.* **2013**, *3*, 3581.
(9) Trasatti, S. *Electrochim. Acta* **1987**, *32*, 843.
(10) Kelly, C. P.; Cramer, C. J.; Truhlar, D. G. *J. Phys. Chem. B* **2006**, *110*, 16066.
(11) Kelly, C. P.; Cramer, C. J.; Truhlar, D. G. *J. Phys. Chem. B* **2007**, *111*, 408.
(12) Isse, A. A.; Gennaro, A. *J. Phys. Chem. B* **2010**, *114*, 7894.
(13) Reiss, H.; Heller, A. *J. Phys. Chem.* **1985**, *89*, 4207.
(14) Fawcett, R. W. *Langmuir* **2008**, *24*, 9868.
(15) Donald, W. A.; Leib, R. D.; Jeremy, T.; O'Brien, J. T.; Williams, E. R. *Chem.—Eur. J.* **2009**, *15*, 5926.
(16) Davis, A. P.; Fry, A. J. *J. Phys. Chem. A* **2010**, *114*, 12299.
(17) Donald, W. A.; Leib, R. D.; O'Brien, J. T.; Bush, M. F.; Williams, E. R. *J. Am. Chem. Soc.* **2008**, *130*, 3371.
(18) Matsui, T.; Kitagawa, Y.; Okumura, M.; Shigeta, Y.; Sakaki, S. *J. Comput. Chem.* **2013**, *34*, 21.
(19) Matsui, T.; Oshiyama, A.; Shigeta, Y. *Chem. Phys. Lett.* **2011**, *502*, 248.
(20) Matsui, T.; Miyachi, H.; Baba, T.; Shigeta, Y. *J. Phys. Chem. A* **2011**, *115*, 8504.
(21) Matsui, T.; Baba, T.; Kamiya, K.; Shigeta, Y. *Phys. Chem. Chem. Phys.* **2012**, *14*, 4181.
(22) Roy, L. E.; Jakubikova, E.; Guthrie, M. G.; Batista, E. R. *J. Phys. Chem. A* **2009**, *113*, 6745.
(23) Solis, B. H.; Hammes-Schiffer, S. *J. Am. Chem. Soc.* **2012**, *134*, 15253.
(24) Hughes, T. F.; Friesner, R. A. *J. Chem. Theory Comput.* **2012**, *8*, 442.

(25) Hughes, T. F.; Friesner, R. A. *J. Chem. Theory Comput.* **2011**, 7, 19.

(26) Klamt, A.; Schüürmann, G. *J. Chem. Soc., Perkin Trans.* **1993**, 2, 799.

(27) Barone, V.; Cossi, M. *J. Phys. Chem. A* **1998**, 102, 1995.

(28) Cancès, M. T.; Mennucci, B.; Tomasi, J. *J. Chem. Phys.* **1997**, 107, 3032.

(29) Mennucci, B.; Tomasi, J. *J. Chem. Phys.* **1997**, 106, 5151.

(30) Pecsok, R. L.; Shields, L. D.; Schaefer, W. P. *Inorg. Chem.* **1964**, 3, 114.

(31) Schaefer, W. P. *Inorg. Chem.* **1965**, 4, 642.

(32) Milazzo, G.; Caroli, S. *Tables of Standard Electrode Potentials*; John Wiley & Sons, Ltd.: New York, 1978.

(33) Ogino, H.; Ogino, K. *Inorg. Chem.* **1983**, 22, 2208.

(34) Bard, A. J.; Parsons, R.; Jordan, J. *Standard Potentials in Aqueous Solution*; Marcel Dekker, Inc.: New York, 1985.

(35) Krüger, H.-J.; Holm, R. H. *J. Am. Chem. Soc.* **1990**, 112, 2955.

(36) Sharpe, P.; Richardson, D. E. *J. Am. Chem. Soc.* **1991**, 113, 8339.

(37) Guldi, D.; Wasgestian, F.; Meyerstein, D. *Inorg. Chim. Acta* **1992**, 194, 15.

(38) Hecht, M.; Schultz, F. A.; Speiser, B. *Inorg. Chem.* **1996**, 35, 5555.

(39) Hecht, M.; Fawcett, W. R. *J. Phys. Chem.* **1996**, 100, 14240.

(40) Ward, M. S.; Shepherd, R. E. *Inorg. Chim. Acta* **1999**, 286, 197.

(41) Fu, Y.; Cole, A. S.; Swaddle, T. W. *J. Am. Chem. Soc.* **1999**, 121, 10410.

(42) Basallote, M. G.; Bernhardt, P. V.; Calvet, T.; Castillo, C. E.; Font-Bardia, M.; Martínez, M.; Rodríguez, C. *Dalton Trans.* **2009**, 9567.

(43) Brausam, A.; Maigut, J.; Meier, R.; Szilágyi, P. A.; Buschmann, H.-J.; Massa, W.; Homonnay, Z.; van Eldik, R. *Inorg. Chem.* **2009**, 48, 7864.

(44) Lord, R. L.; Schultz, F. A.; Baik, M.-H. *J. Am. Chem. Soc.* **2009**, 131, 6189.

(45) Siburt, C. J. P.; Lin, E. M.; Brandt, S. J.; Tinoco, A. D.; Valentine, A. M.; Crumbliss, A. L. *J. Inorg. Biochem.* **2010**, 104, 1006.

(46) Frisch, M. J.; Trucks, G. W.; Schlegel, H. B.; Scuseria, G. E.; Robb, M. A.; Cheeseman, J. R.; Scalmani, G.; Barone, V.; Mennucci, B.; Petersson, G. A.; Nakatsuji, H.; Caricato, M.; Li, X.; Hratchian, H. P.; Izmaylov, A. F.; Bloino, J.; Zheng, G.; Sonnenberg, J. L.; Hada, M.; Ehara, M.; Toyota, K.; Fukuda, R.; Hasegawa, J.; Ishida, M.; Nakajima, T.; Honda, Y.; Kitao, O.; Nakai, H.; Vreven, T.; Montgomery, J. A., Jr.; Peralta, J. E.; Ogliaro, F.; Bearpark, M.; Heyd, J. J.; Brothers, E.; Kudin, K. N.; Staroverov, V. N.; Kobayashi, R.; Normand, J.; Raghavachari, K.; Rendell, A.; Burant, J. C.; Iyengar, S. S.; Tomasi, J.; Cossi, M.; Rega, N.; Millam, J. M.; Klene, M.; Knox, J. E.; Cross, J. B.; Bakken, V.; Adamo, C.; Jaramillo, J.; Gomperts, R.; Stratmann, R. E.; Yazyev, O.; Austin, A. J.; Cammi, R.; Pomelli, C.; Ochterski, J. W.; Martin, R. L.; Morokuma, K.; Zakrzewski, V. G.; Voth, G. A.; Salvador, P.; Dannenberg, J. J.; Dapprich, S.; Daniels, A. D.; Farkas, Ö.; Foresman, J. B.; Ortiz, J. V.; Cioslowski, J.; Fox, D. J. *Gaussian 09*, revision C.01; Gaussian, Inc.: Wallingford, CT, 2009.

(47) Becke, A. D. *J. Chem. Phys.* **1993**, 98, 5648.

(48) Perdew, J. P.; Burke, K.; Ernzerhof, M. *Phys. Rev. Lett.* **1996**, 77, 3865.

(49) Iikura, H.; Tsuneda, T.; Yanai, T.; Hirao, K. *J. Chem. Phys.* **2001**, 115, 3540.

(50) Song, J.-W.; Hirosawa, T.; Tsuneda, T.; Hirao, K. *J. Chem. Phys.* **2007**, 126, 154105.

(51) Zhao, Y.; Truhlar, D. G. *Theor. Chem. Acc.* **2008**, 120, 215.

(52) Roy, L. E.; Hay, P. J.; Martin, R. L. *J. Chem. Theory Comput.* **2008**, 4, 1029.

(53) Wachters, A. J. H. *J. Chem. Phys.* **1970**, 52, 1033.

(54) Bauschlicher, C. W., Jr.; Langhoff, S. R.; Barnes, L. A. *J. Chem. Phys.* **1989**, 91, 2399.

(55) Balabanov, N. B.; Peterson, K. A. *J. Chem. Phys.* **2005**, 123, 064107.

(56) McNamara, W. R.; Han, Z.; Yin, C.-J.; Brennessel, W. W.; Holland, P. L.; Eisenberg, R. *Proc. Natl. Acad. Sci. U. S. A.* **2012**, 109, 15594.

(57) Kaim, W. *Inorg. Chem.* **1984**, 23, 504.

(58) Geiger, W. E.; Senftleber, F. C. *J. Am. Chem. Soc.* **1975**, 97, 5018.

(59) Connelly, N. G.; Geiger, W. E. *Chem. Rev.* **1996**, 96, 877.

(60) Saji, T.; Aoyagui, S. *J. Electroanal. Chem.* **1975**, 60, 1.

(61) Tsuneda, T.; Song, J.-W.; Suzuki, S.; Hirao, K. *J. Chem. Phys.* **2010**, 133, 174101.

2980

dx.doi.org/10.1021/ct4002653 | *J. Chem. Theory Comput.* 2013, 9, 2974−2980